

Geophysical Research Letters

Supporting Information for

Impact of ENSO-like tropical Pacific decadal variability on the relative frequency of El Niño and La Niña events

Tianyi Sun[†], and Yuko M. Okumura

Institute for Geophysics, Jackson School of Geosciences, University of Texas at Austin, Austin, Texas

Corresponding author: Tianyi Sun (tsun@edf.org)

[†] Current affiliation: Environmental Defense Fund, NY 10010. Address: 301 Congress Ave., Austin, TX 78701.

Contents of this file

Table S1 and Figures S1 to S9

Introduction

This Supplementary Information contains 1 table and 9 figures to complement the model experiment results presented in the main text. Table S1 shows the number of ENSO events categorized by the preceding conditions in the CCSM4-CTL and TPDV1-P/N experiments. Figures S1 and S2 present the mean state and ENSO response to surface heat flux forcing for one standard deviation of TPDV PC1. Figures S3-9 present supplemental results of the TPDV1-P/N experiments discussed in the main text. Figure S3 shows the mean state response in individual ensemble members. The seasonality of the mean state response is presented in Figures S4 and S5. Figures S6 and S7 examine ocean-atmosphere anomalies associated with the development of ENSO events in the CCSM4-CTL and compare them to the mean state response in the TPDV1-P/N experiments. Figure S8 compares ocean mixed layer heat budget for El Niño and La Niña between the CCSM4-CTL and TPDV1-P/N experiments. Figure S9 shows ENSO response based on the climatology of the TPDV1-P/N experiments.

	El Niño	Year -1			Year -1	
		La Niña	Neutral	La Niña	El Niño	Neutral
CCSM4-CTL	14	0.5	13.5	14	6.1	7.9
TPDV1-P	20.7	1	19.7	9.3	6	3.3
TPDV1-N	8.7	1	7.7	14.3	3.7	10.6

Table S1. The average numbers of El Niño (La Niña) events per 100 years and those preceded by La Niña (El Niño) or neutral conditions in the previous year for the CCSM4-CTL (first row), TPDV1-P (second row) and TPDV1-N (third row) experiments.

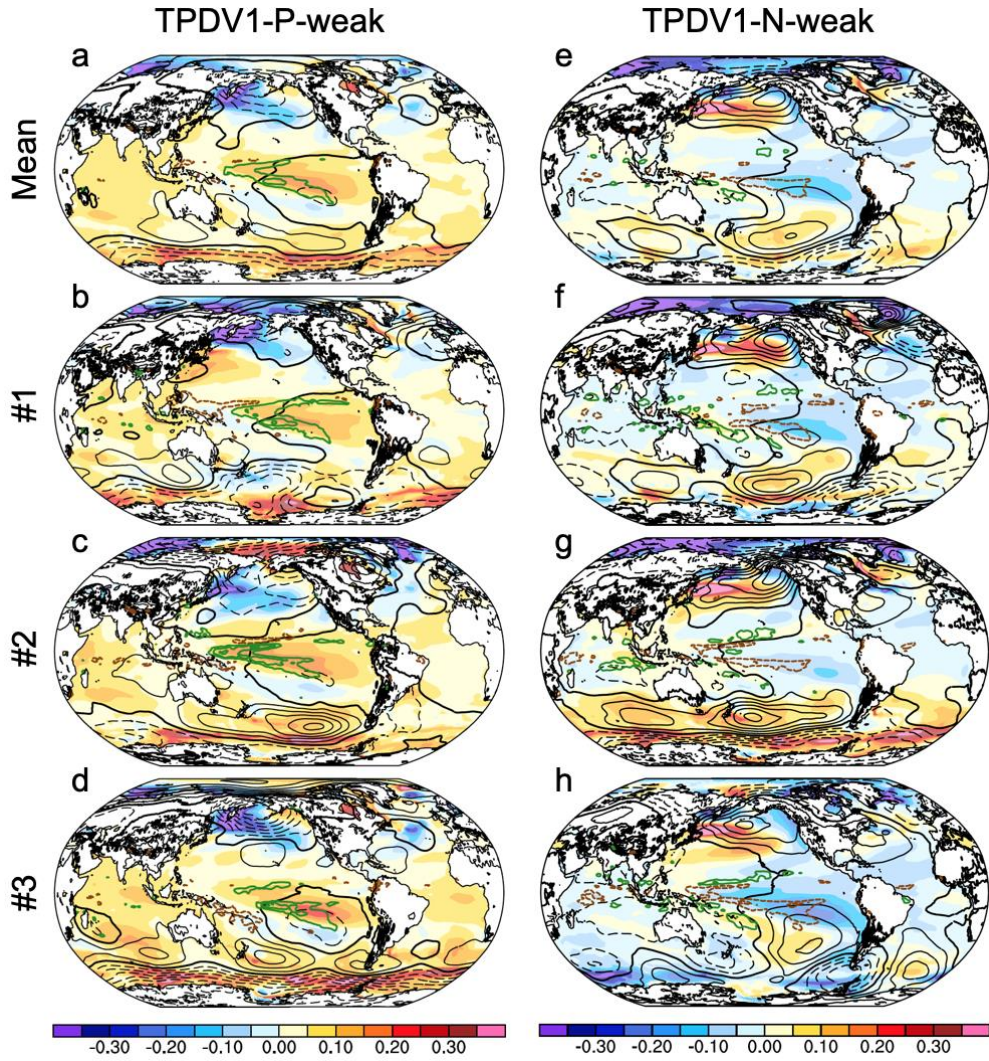


Figure S1. Mean state response to surface heat flux forcing for positive and negative one standard deviation of TPDV PC1. Annual mean response of global surface temperature (shading; °C), SLP (contours at intervals of 0.1 hPa), and precipitation (contours at intervals of 0.2 mm day⁻¹; negative contours dashed and zero contours omitted) in (a, e) the ensemble mean and (b-d, f-h) individual ensemble members of (a-d) the positive and (e-h) negative experiments.

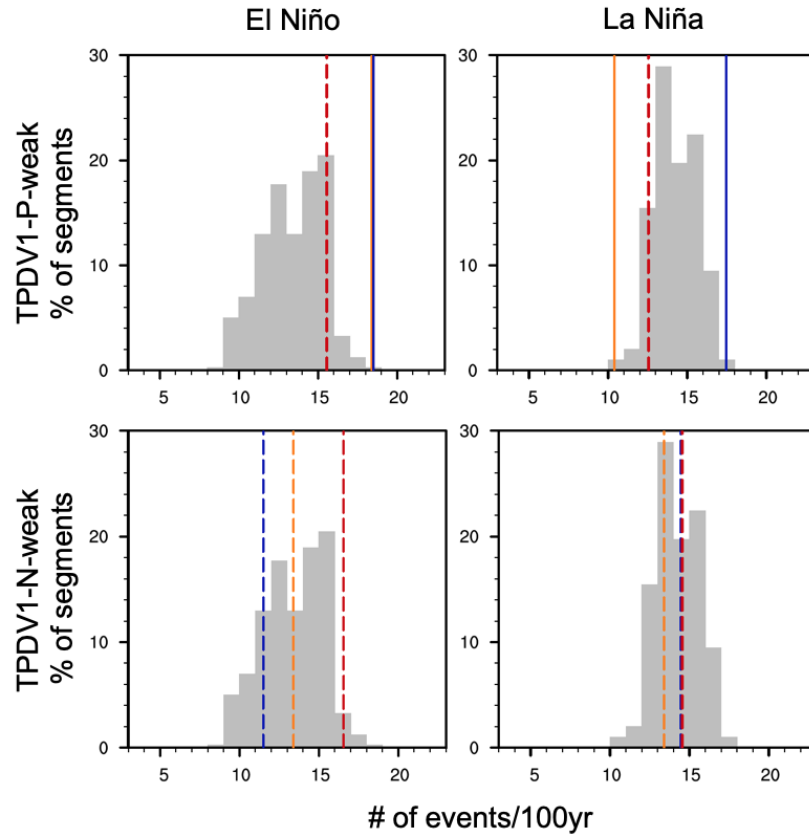


Figure S2. As in Figure 2c-f but for the experiments conducted with surface heat flux forcing for positive and negative one standard deviation of TPDV PC1.

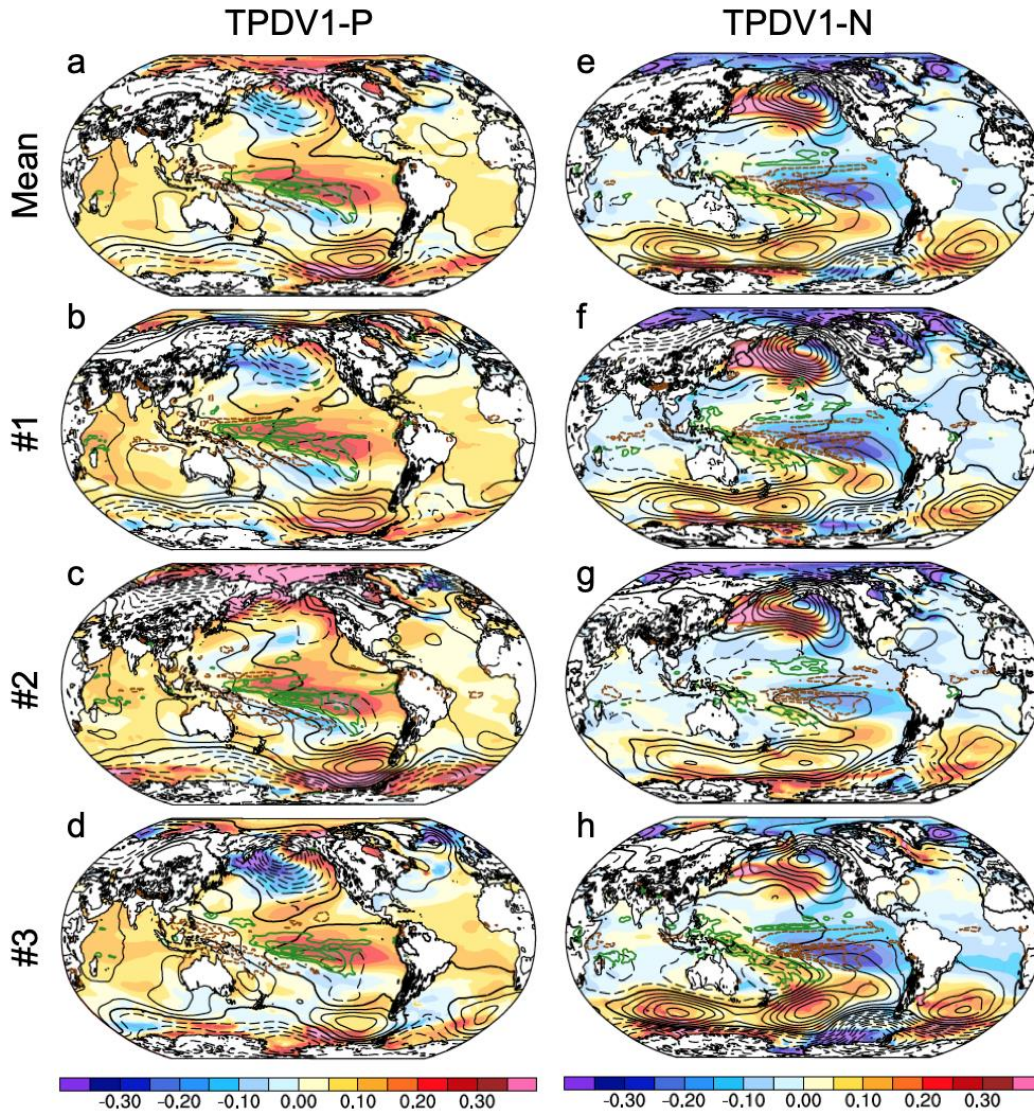


Figure S3. As in Figure S1 but for the TPDV1-P/N experiments.

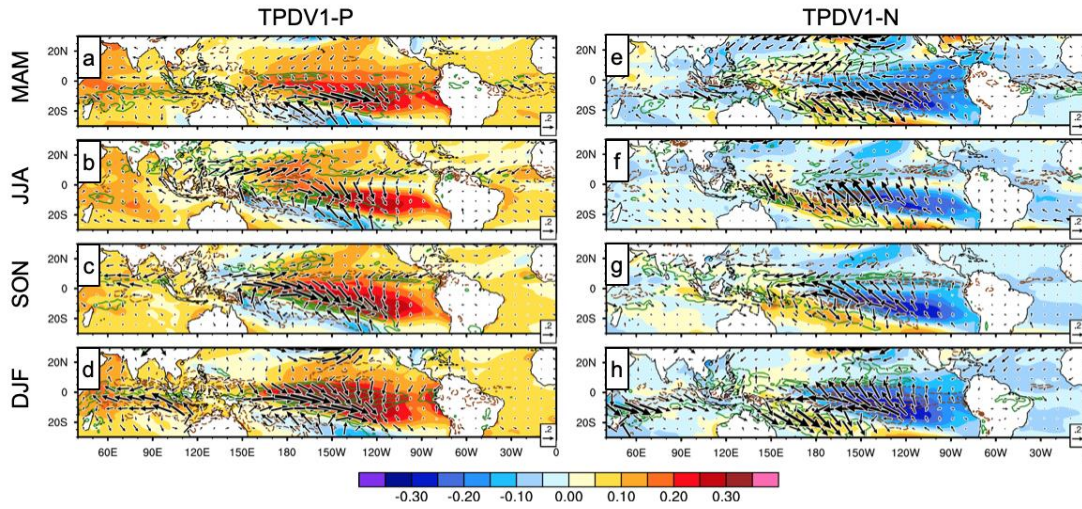


Figure S4. Ensemble mean seasonal response of tropical SST (shading; °C), surface wind (vectors; m s⁻¹), and precipitation (contours at intervals of 0.2 mm day⁻¹; negative contours dashed and zero contours omitted) in (a-d) the TPDV1-P and (e-h) TPDV1-N experiments.

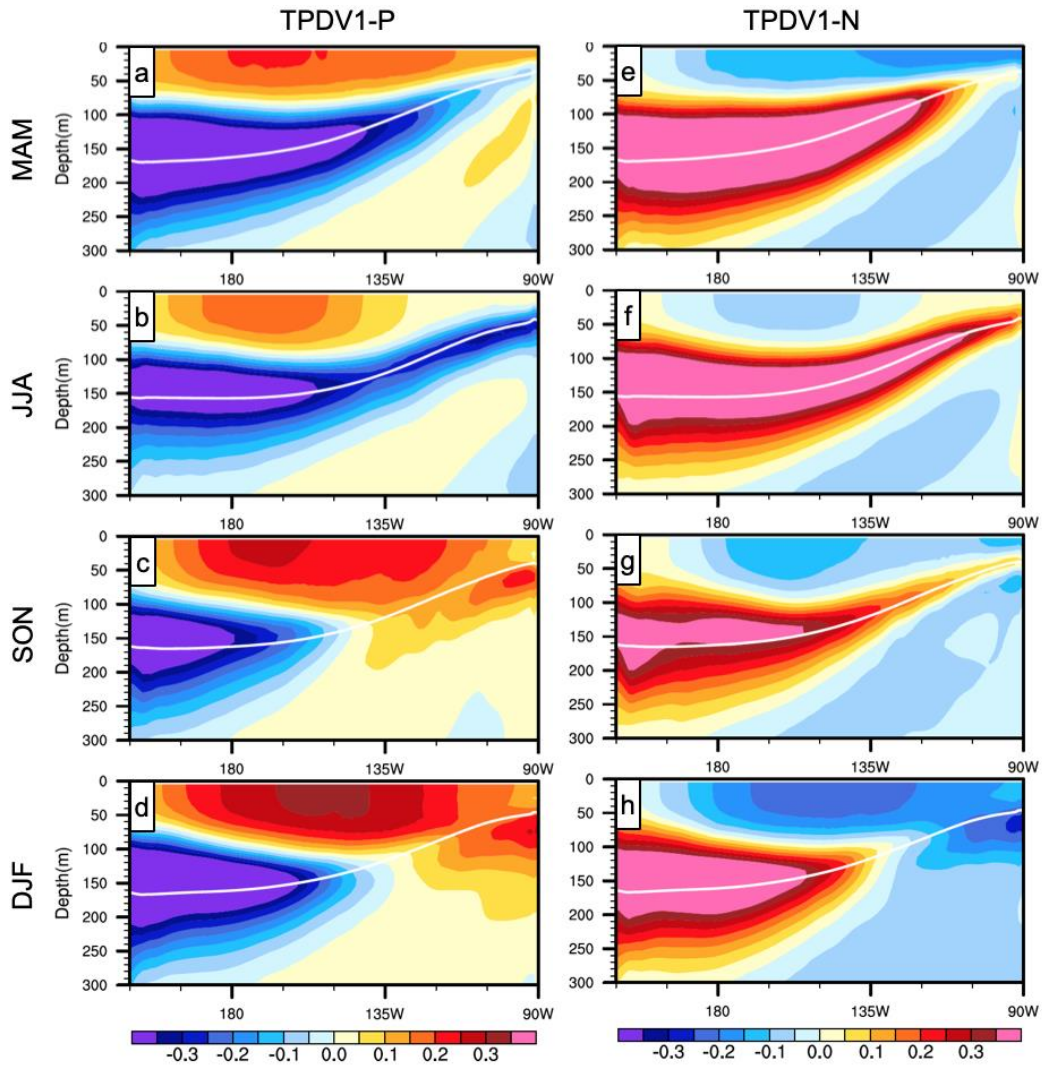


Figure S5. Ensemble mean seasonal response of equatorial Pacific (3°N-3°S) ocean potential temperature (shading; °C) in (a-d) the TPDV1-P and (e-h) TPDV1-N experiments. The white lines denote the climatological isopycnal $\sigma_{\theta} = 25.5 \text{ kg m}^{-3}$ that approximates the thermocline depth in the CCSM4-CTL.

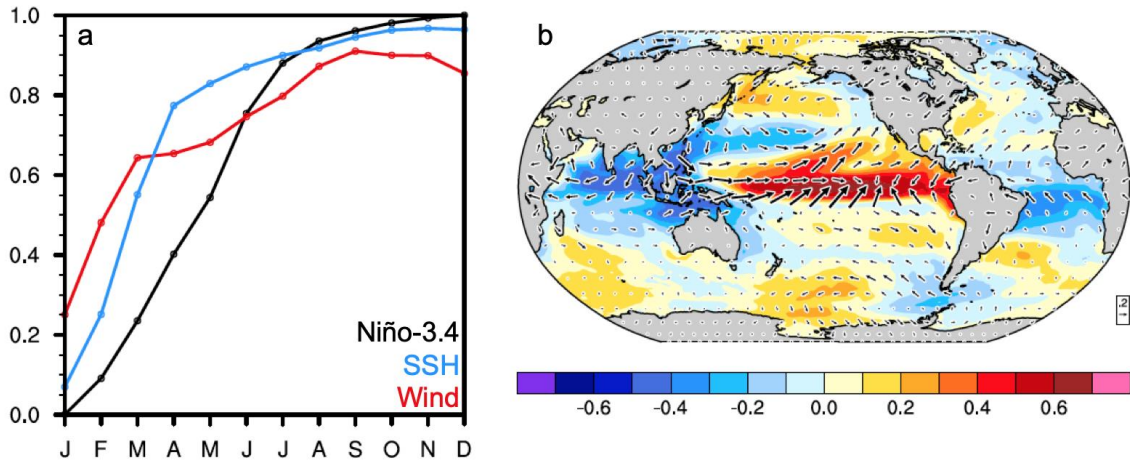


Figure S6. Ocean-atmosphere anomalies related to the development of ENSO events in the CCSM4-CTL. (a) Correlations of the December Niño-3.4 index with the Niño-3.4 index (black), SSH in the eastern equatorial Pacific (5°S – 5°N , 150° – 80°W ; blue), and surface zonal wind in the western equatorial Pacific (5°S – 5°N , 130° – 180°E ; red) for months of the same year. (b) Correlation map of February–April global surface temperature (shading) and surface wind (vectors) anomalies with the December Niño-3.4 index of the same year. One-sided regressions on the December Niño-3.4 index of the previous year are removed from the February–April surface temperature and wind fields prior to the correlation analysis. See Okumura et al. (2017a) for further discussions.

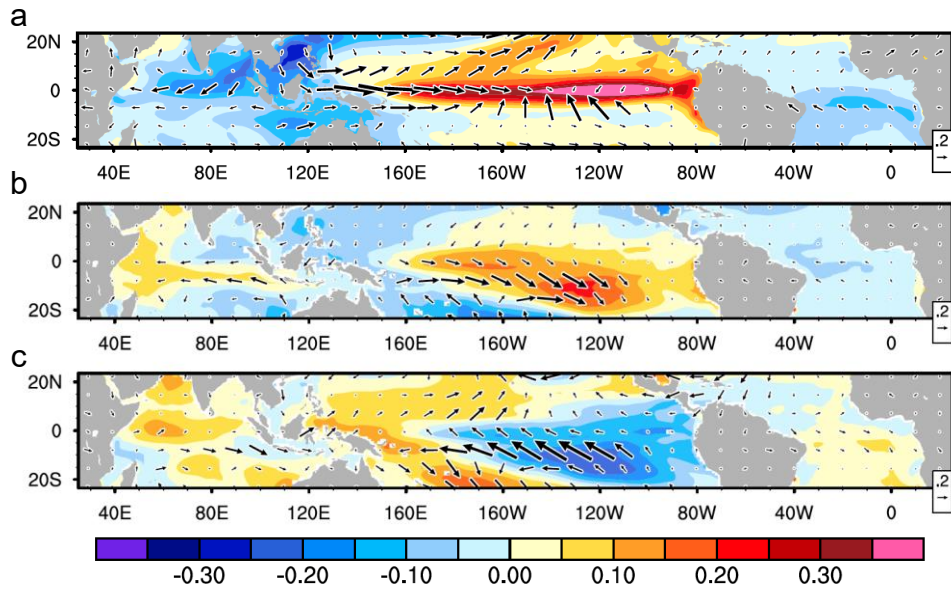


Figure S7. (a) Regression map of February–April tropical SST (shading; °C) and surface wind (vectors; m s⁻¹) anomalies with the December Niño-3.4 index of the same year. The regression anomalies are for one standard deviation of the December Niño-3.4 index. One-sided regressions on the December Niño-3.4 index of the previous year are removed from the February–April surface temperature and wind fields prior to the regression analysis. (b, c) Maps of February–April mean changes in (c, e) T-T* (shading; °C) and surface wind (vectors; m s⁻¹) in (b) the TPDV1-P and (c) TPDV1-N experiments.

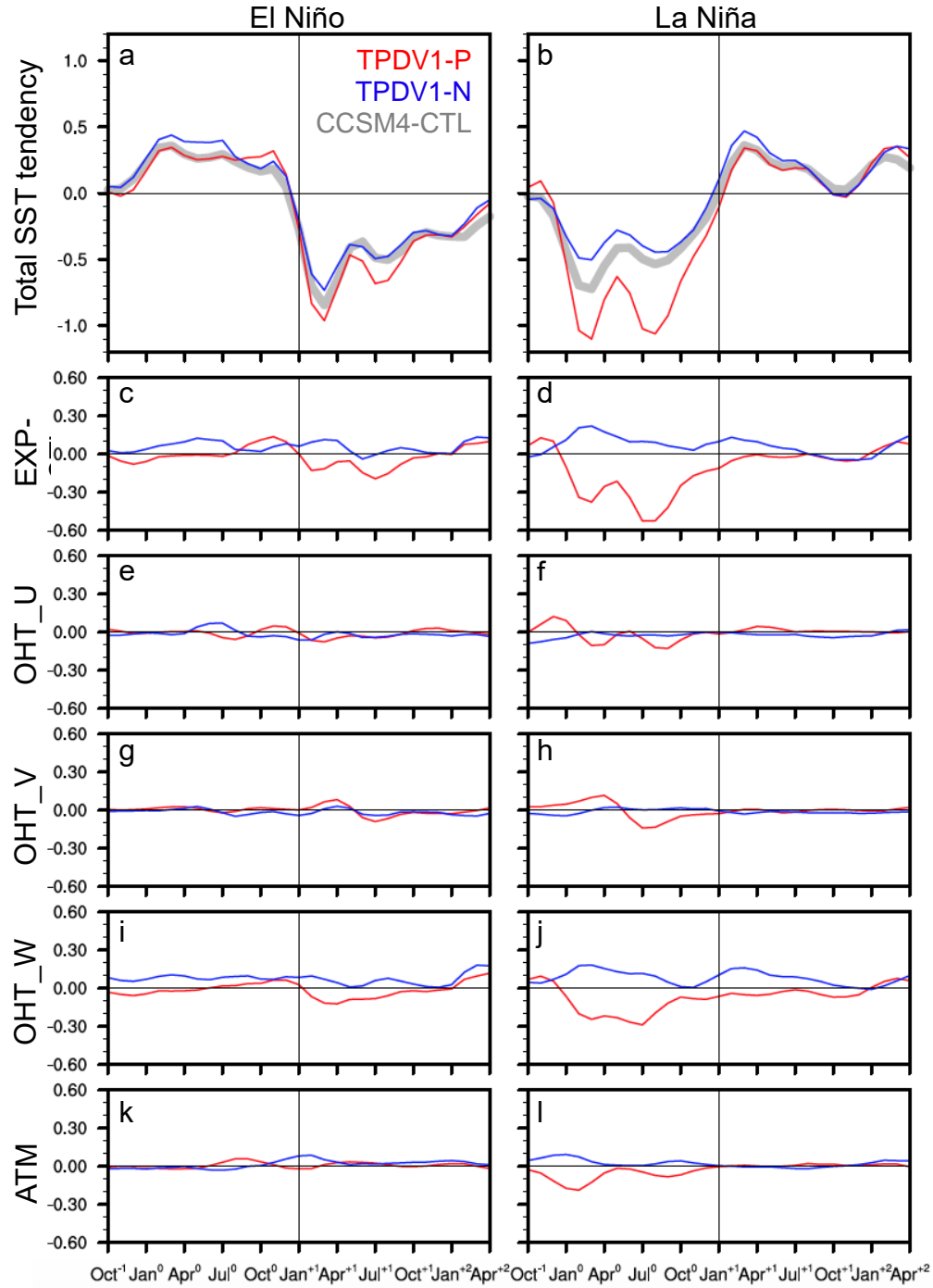


Figure S8. Changes in the ocean mixed layer heat budget during ENSO events in the TPDV1-P/N experiments. (a, b) Composite evolution of Niño-3.4 SST tendencies ($K \text{ month}^{-1}$) for (a) El Niño and (b) La Niña in the TPDV1-P (red) and TPDV1-N (blue) experiments and CCSM4-CTL (gray). (c-l) Differences in (c) the El Niño and (d) La Niña composites between the TPDV1-P/N experiments and CCSM4-CTL (red/blue). These differences are further decomposed into contributions from (e, f) zonal, (g, h) meridional, and (i, j) vertical ocean heat transport and (k, l) net surface heat flux (downward positive). All heat budget terms are calculated for the ocean mixed layer in the Niño-3.4 region (5°S – 5°N , 170° – 120°W).

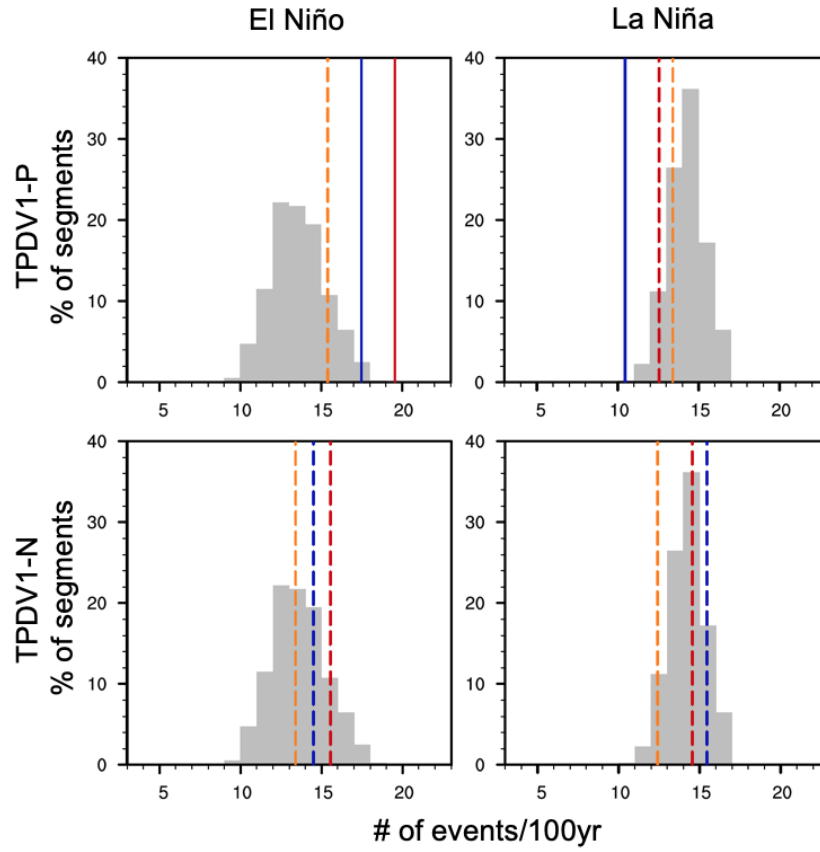


Figure S9. As in Figure 2c-f, but ENSO events are defined based on the climatology of individual ensemble members of the TPDV1-P/N experiments and individual 100-yr segments of the CCSM4-CTL.